NUMERICAL ANALYSIS OF FREE CONVECTIVE HEAT TRANSFER IN VERTICAL DUCT WITH LAMINAR UPFLOW

YU-TIEN HSIAO, TAMOTSU HANZAWA AND NOBORU SAKAI

Department of Food Engineering, Tokyo University of Fisheries, Tokyo 108

Key Words: Heat Transfer, Heat Transfer Coefficient, Free-Forced Convection, Combined Laminar Flow, Combined Flow Pattern

To elucidate the heat transfer phenomena for a package in a refrigerating room with upflow, we considered a vertical-duct model in which one wall was isothermally heated and gas flowed upward through the duct in the laminar-flow range. The velocity profiles, temperature distributions and the local and average heat transfer coefficient were calculated numerically by fundamental equations.

The main fluid flow is drawn toward the heated wall in the range of low *Re* and becomes parallel to the axial coordinate with increasing *Re*. The higher on the heated wall, the smaller is the local Nusselt number. However, the average Nusselt number does not undergo much change with increasing *Re* and *Gr*. A correlated equation for heat transfer was obtained under the operating conditions of this calculation.

To check these calculated results, the temperature distributions and heat transfer coefficient were measured experimentally under the same operating conditions as those of the theoretical analysis. The calculated temperature distributions agreed closely with the measured ones.

To compare the heat transfer coefficient of the downflow and the upflow, we found that the latter is about twice that of the former.

Introduction

Generally, when a food package is put into a refrigerating room for storage the density of fluid near the package wall is lowered by the temperature rise and free convection is generated. The free convection promotes heat transfer from the package wall to ambient fluid. In the refrigerating room, cold fluid flows through the space between the packages in the laminar flow range, and free convection is combined with this laminar forced convection.

In previous studies, downward forced convective flow was weakened by the free convective flow, and a stagnant flow arose in the low Reynolds number range ($Re = 300 - 1500$) in such a room. It was proved that the rate of heat transfer from the package wall in the refrigerating room decreased with increasing flow rate of the cold fluid in the downflow. Therefore, it seems that in the case of upward flow the heat transfer rate is larger than that of downward flow.

Numerical studies of fluid flow in a normal room have been reported[16, 17], and many experimental and theoretical approaches have been taken to the fluid flow in a refrigerating room and to similar flow systems[1-15, 18]. However, there are few works concerning the problem of combined free-forced convective laminar flow between the packages[5, 6]. Thus the combined convective heat transfer from the package wall in a refrigerating room is not yet established as to heat transfer coefficients under various operating conditions. Such information is important for energy saving.

In this study, as basic research on the effect of direction of cold fluid flow on the cooling of the package, the temperature distributions and heat transfer coefficients for a vertical duct wall at a constant temperature were measured and solved numerically in the case where only one side-wall of the duct was heated and gas flowed upward through the duct in the laminar flow range. This is a model of the package wall in a refrigerating room in which the temperature differences between the package wall and the ambient cold fluid are the same as those between a heated wall and a flowing gas of normal temperature in the duct.

A correlative equation for the coefficients of heat transfer from the isothermally heated wall in the duct was obtained by taking account of the Reynolds number, the Grashof number and the geometrical conditions of the vertical duct for combined free-forced convective laminar flow. Also, the heat transfer coefficients determined in this study were compared with those in the literature[3, 4, 12] and with those in the case of downward flow[5, 6].

1. Fundamental Equations and Numerical Calculations

From observation of the flow pattern ($TiCl_4$ tracer) in a preliminary experiment, it seems reasonable to ana

* Received October 7, 1992. Correspondence concerning this article should be addressed to T. Hanzawa.

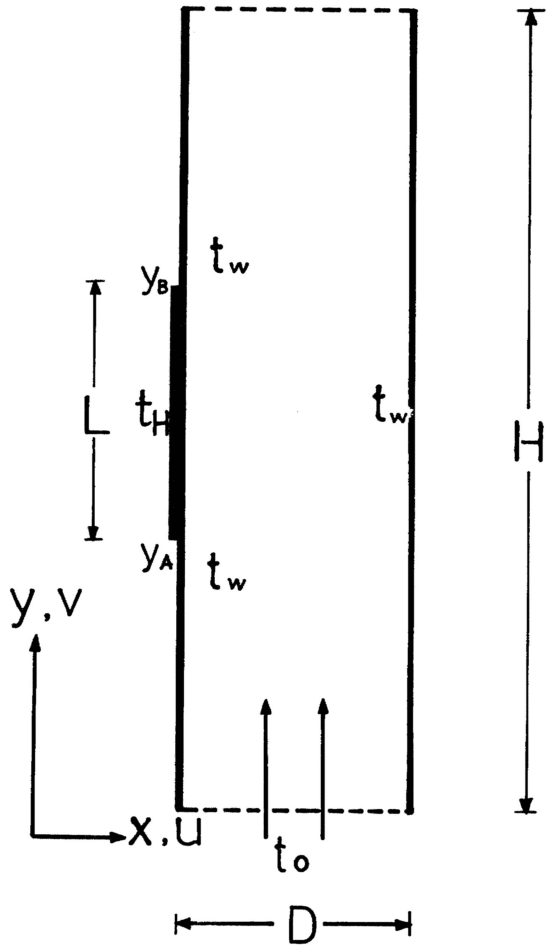

Fig. 1 Coordinate system for a vertical duct

Table 1. Grid size and number of iterations

ΔX	ΔY	Number of iterations
0.0191-0.05	0.0326-0.18	200-2000

lyze the transport phenomena by considering two-dimensional flow in the vertical cross section. Let us consider the heat transfer phenomenon with combined free and forced laminar convection in a duct, where a part of one side-wall is heated and the other side-wall is kept at a constant temperature, as shown in **Fig. 1.**

If it is assumed that the physical properties of the fluid are constant and independent of temperature, that the buoyancy is directly proportional to the temperature difference, that the velocity derivatives in the direction of depth is neglected, and that air feed into an entrance region of the test section with a velocity profile of plug flow and velocity component symmetrical to the axial direction in an exit region, the dimensionless fundamental equations and boundary conditions are obtained as follows:

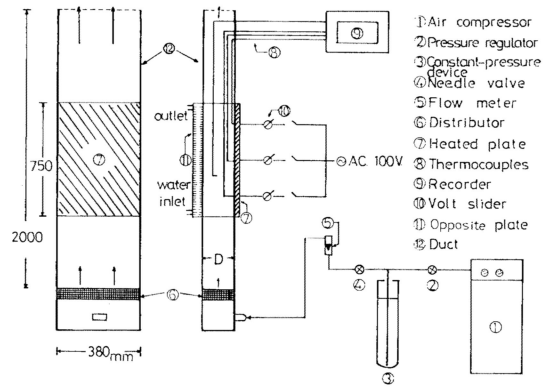

Fig. 2 Experimental apparatus

$$\frac{\partial U}{\partial X}+\frac{\partial V}{\partial Y}=0 \tag{1}$$

$$U\frac{\partial U}{\partial X}+V\frac{\partial U}{\partial Y}+\frac{\partial P}{\partial X}=\left(\frac{\partial^2 U}{\partial X^2}+\frac{\partial^2 U}{\partial Y^2}\right) \tag{2}$$

$$U\frac{\partial V}{\partial X}+V\frac{\partial V}{\partial X}+\frac{\partial P}{\partial Y}=\left(\frac{\partial^2 V}{\partial X^2}+\frac{\partial^2 V}{\partial Y^2}\right)-Gr\cdot T \tag{3}$$

$$U\frac{\partial T}{\partial X}+V\frac{\partial T}{\partial Y}=\frac{1}{Pr}\left(\frac{\partial^2 T}{\partial X^2}+\frac{\partial^2 T}{\partial Y^2}\right) \tag{4}$$

(boundary conditions)

$$\left.\begin{aligned} &X=0,\begin{cases}0\le Y<Y_A,\ Y_B<Y\le Y_H;\ U=V=0,\ T=T_w\\ Y_A\le Y\le Y_B;\ U=V=0,\ T=1\end{cases}\\ &X=1;\ U=V=0,\ T=T_W\\ &Y=0;\ U=0,\ V=V_0,\ T=0\\ &Y=Y_H;\ \frac{\partial U}{\partial Y}=\frac{\partial V}{\partial Y}=\frac{\partial T}{\partial Y}=0\end{aligned}\right\} \tag{5}$$

The dimensionless stream function ψ and vorticity ξ were introduced to Eqs. (1)-(4) and each equation was written in a finite difference form by the "upwind method". They were then solved numerically by a relaxation method.

The optimum values of the relaxative condition were found by trial and error for a given system of grid points. Representative values of grid size and the iteration number for good convergence are given in **Table 1.**

These calculations were performed over the ranges Re = 100 – 2500, $Gr = 3.02\times10^5 - 2.2\times10^7$, Pr = 0.7 and L/D = 5 – 15 (D = 5, 8, 10, 12, 15 cm, L = 75.0 cm).

2. Experimental Apparatus and Procedure

To check the calculated results, the temperature distributions in the duct were measured.

Figure 2 shows a schematic diagram of the experi-

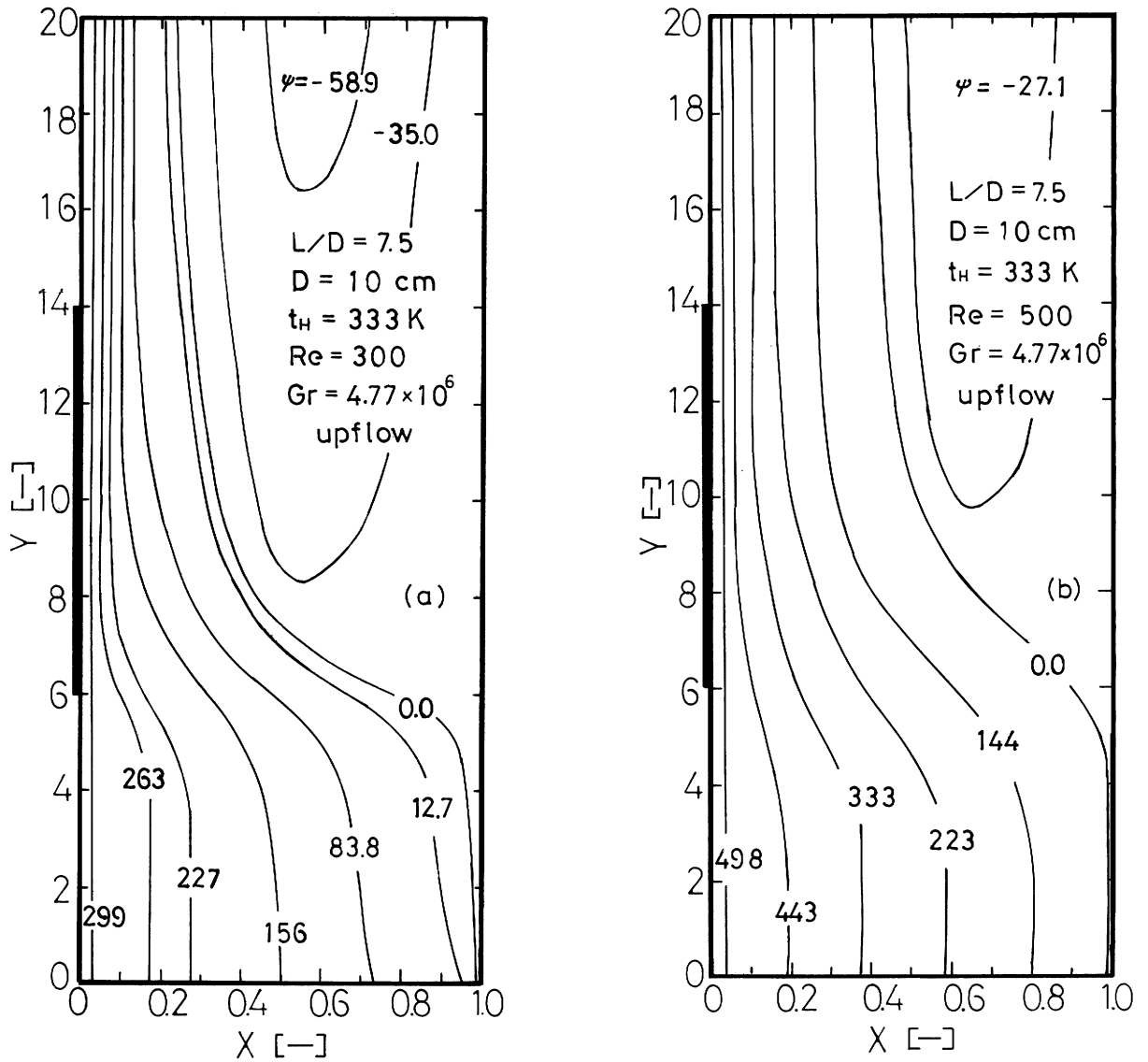

Fig. 3 Streamline with Re = 300, 500, 1200 for t_H = 333 K and L/D = 7.5

mental apparatus. The ducts, main section of the system, with a cross-sectional area of 38 × 15 cm^2, 38 × 12 cm^2, 38 × 10 cm^2, 38 × 8 cm^2, and 38 × 5 cm^2, and 200 cm in length including the entrance region, were made of acrylic resin. The heating section was located in the middle of the duct and its area was 38 (width) × 75 (height) cm^2. The heating section consisted of a copper plate in which nichrome wires were placed as heaters at three locations and were heated individually to obtain the isothermal condition. The opposite plate was not heated, and a water jacket was attached to it to obtain the isothermal condition. The sectional area of the duct was changed by moving this opposite plate.

To measure the temperature in the test section, CC thermocouples (0.5 mm ϕ) were placed at nine points in the heated wall and at three points in the opposite wall.

Thus, it was found that the wall temperatures of the heated plate and of the opposite plate were nearly uniform. Furthermore, the wall temperatures of the opposite plate except those of the water jacket were also measured by thermocouples and it was found that the temperature difference between the wall of the water jacket and that of the opposite plate itself was negligibly small.

To investigate correctly the cross-sectional temperature distribution in the boundary layer and the fluid in the duct, gas temperature was measured by use of a sheathed CA thermocouple probe of very small diameter (0.2 mm ϕ) and the cross-sectional spacing for measurement was 0.5 mm in the boundary layer and 10.0 mm in the ambient fluid.

Regulated air was fed into the test section from the bottom of the duct and then the sheathed thermocouple probe was traversed in the cross section by moving the slider to measure the local temperature in the duct. The flow rate of air was in the range of Re = 100 to 2500. The experimental procedure was almost the same as that described in the previous paper[5, 6].

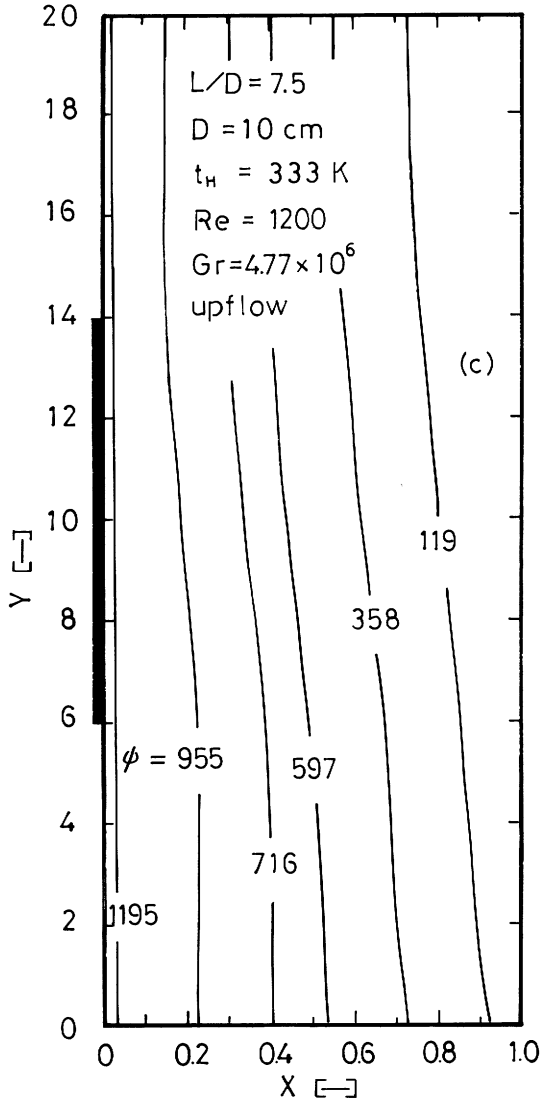

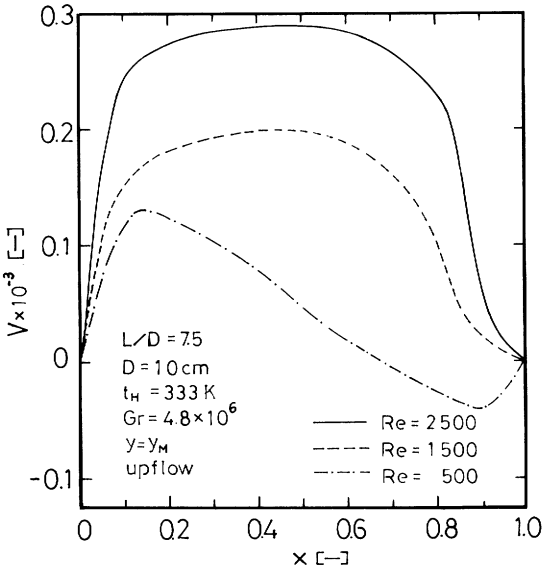

Fig. 4 Effect of *Re* on calculated axial velocity profile

3. Calculation Results and Comparison of Calculated with Experimental Values

3.1 Streamline and velocity profile

Figure 3 shows some typical streamlines obtained numerically in the vertical cross section through the duct for the cases where the Reynolds numbers were 300, 500 and 1200 respectively for $L/D = 7.5$ ($D = 10$ cm) and $t_H = 333$ K. The abscissa of the figure, X, represents the dimensionless cross-sectional distance from the surface of the heated wall, the ordinate, Y, represents the dimensionless longitudinal distance from the bottom of the test section, and the thick solid line at the left side of the figure represents the heated wall in the duct.

From Fig. 3, at $Re = 300$ and $Re = 500$, the bulk flow is bent intensely from its own current path toward the heated wall by the free convective flow. A similar fluid motion was observed for the flow pattern of a $TiCl_4$ tracer as well. From this figure, it is assumed that the free convective flow generated near the heated wall is stronger than the forced convective flow at $Re = 300$ and 500.

On the other hand, at $Re = 1200$ the bulk flow becomes smooth and approaches parallel flow. It is assumed that the intensity of the forced convective flow becomes almost the same as that of the free convective flow, and in this case it can be considered that there is no effect of the free convective flow. The effect of Reynolds number on the streamlines was observed at other valves of *Gr* and *L/D*.

Figure 4 shows some typical axial velocity profiles at the middle point of the heated wall ($y = y_M$) for $L/D = 7.5$ and $t_H = 333$ K with *Re* as a parameter. In this figure, the plus or minus value of the dimensionless velocity component indicates the direction of this velocity.

From Fig. 4, it is seen that the axial velocity takes its maximum on the side of the heated wall by the effect of free convection. The effect of free convection upon the velocity profile is notable at low *Re*. Since at $Re = 500$ the free convection is more intense than the forced convection, a vortex with back flow arises near the opposite wall.

3.2 Temperature distribution

Figure 5 shows dimensionless temperature distributions in the vertical cross section for the cases where $Re = 300$ and 1200, respectively, and this figure can be related to the streamlines shown in Fig. 3. The axes in this figure are the same as those in Fig. 3, and the solid lines show the temperature distributions calculated from the fundamental equations.

From Fig. 5, as *Re* increases, the temperature gradient near the heated wall is slightly increased, but the shapes of temperature distribution are almost unchanged within the limits of this operating condition. This fact may be explained as follows. Since the effect of free convection on heat transfer is quite large in this range of *Re*, the shapes of the temperature distribution are not much changed even if *Re* is increased.

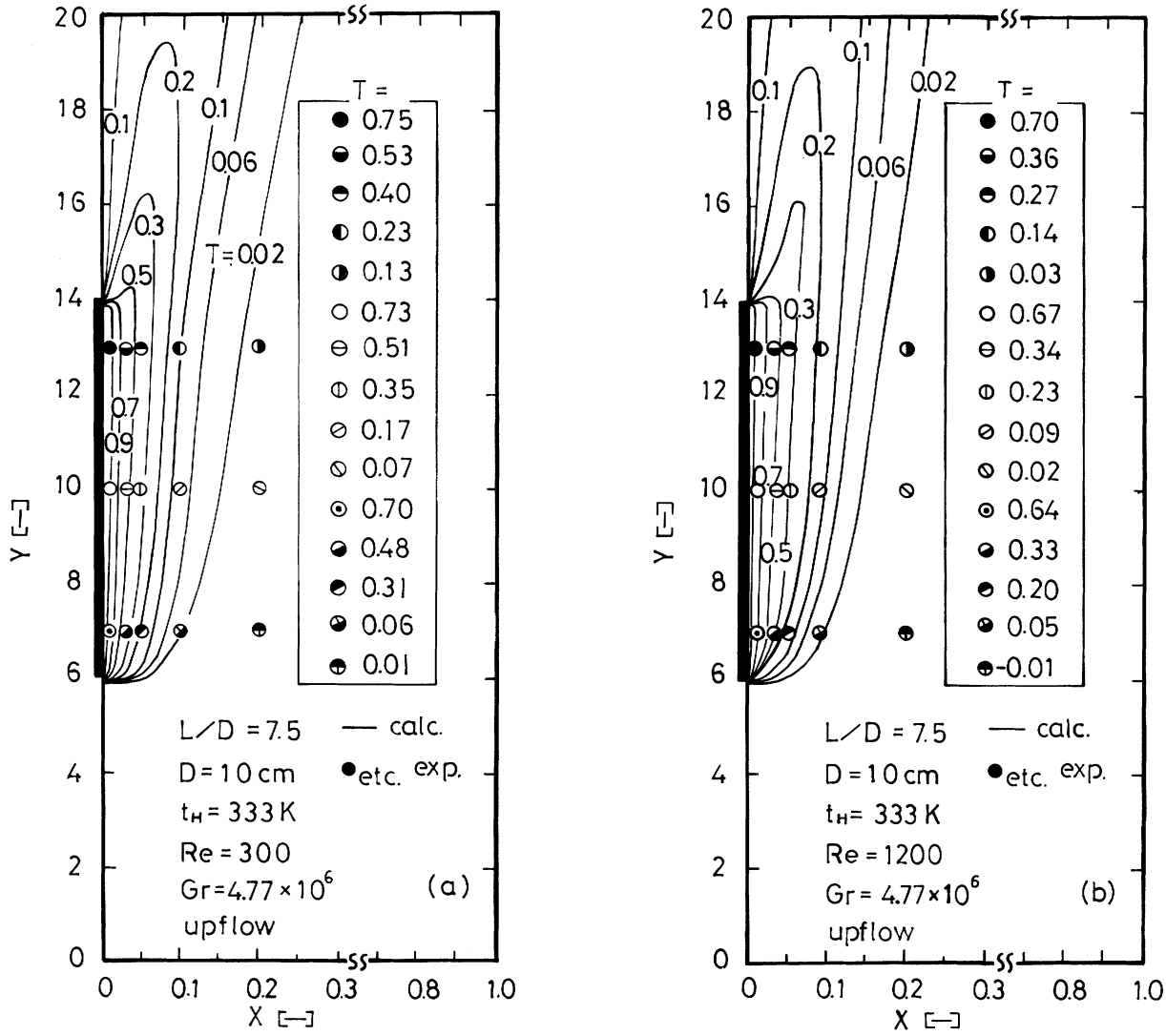

Fig. 5 Temperature distributions with Re = 300, 1200 for t_H = 333 K and L/D = 7.5

In Fig. 5, the plotted points are the dimensionless local temperatures obtained by experiment under the same conditions as those of this numerical calculation. As can be seen from these values, the calculated temperature is a sufficiently good approximation to the measured one.

Figure 6 shows some typical cross-sectional temperature distributions at the middle point of the heated wall ($y = y_M$) for L/D = 7.5, Re = 1200 and L/D = 15.0, Re = 500. The abscissa of this figure represents the dimensionless cross-sectional distance and the ordinate represents the dimensionless temperature, T. The solid lines and the plotted points show calculated values and experimental ones respectively. In Fig. 6 (a), the temperature distribution represents one of those shown in Fig. 5 (b).

From Fig. 6, the temperature gradient becomes steep near the heated wall and is nearly uniform in the ambient fluid. It seems that the calculated values are in sufficiently good agreement with the experimental ones. Such good agreement between calculated results and experimental ones was also obtained in other cases.

3.3 Nusselt number

The local Nusselt number, Nu, and the average one, $\overline{Nu}$, from the heated wall may be obtained by the temperature gradients near the heated wall as follows:

$$Nu = -\left(\frac{\partial T}{\partial X}\right)_{x=0} \tag{6}$$

and

$$\overline{Nu} = \frac{1}{Y_B - Y_A}\int_{Y_A}^{Y_B}\left(\frac{\partial T}{\partial X}\right)_{x=0} dY \tag{7}$$

Figures 7 and **8** show the local Nusselt number on the heated wall in the vertical duct with Re and Gr respectively as parameter. The abscissa in these figures represents the dimensionless longitudinal distance from the bottom of the test section in the duct, the thick solid line represents the heated wall, and each curve in these

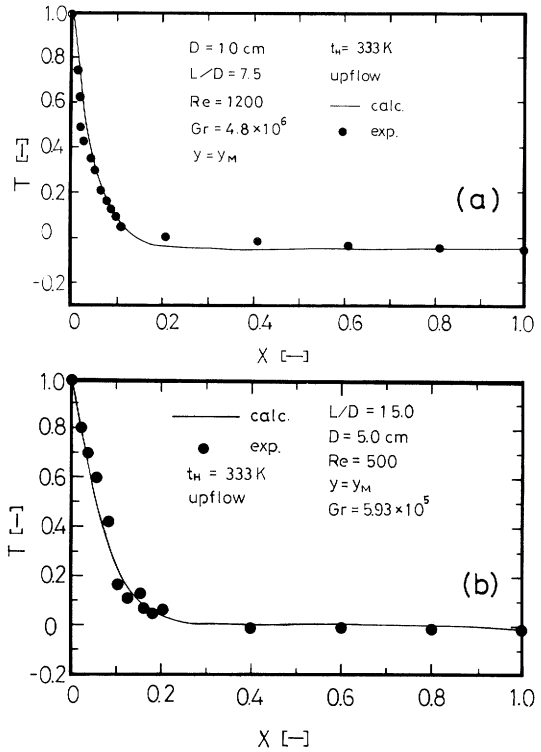

Fig. 6 Comparison of calculated temperature distribution with experimental ones in the cross-sectional direction for L/D = 5.0 and 7.5

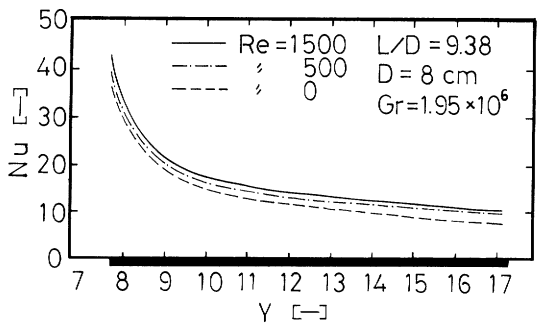

Fig. 7 Effect of *Re* on local Nusselt number

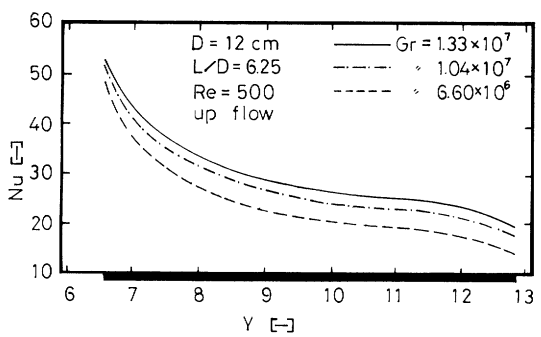

Fig. 8 Effect of *Gr* on local Nusselt number

figures represents the calculated values. From Figs. 7 and 8, *Nu* becomes smaller with increasing *Y*.

In Fig. 7, the effect of *Re* on *Nu* became very small. It seems that the effect of the forced convective flow is very small for heat transfer in this case. This result was also obtained in other cases.

However, in Fig. 8, the effect of *Gr* on *Nu* is noticeable, and *Nu* becoming larger with increasing *Gr*. It seems that the heat transfer is affected very much by the free convective flow, and that the stronger the free convection the larger the heat transfer becomes.

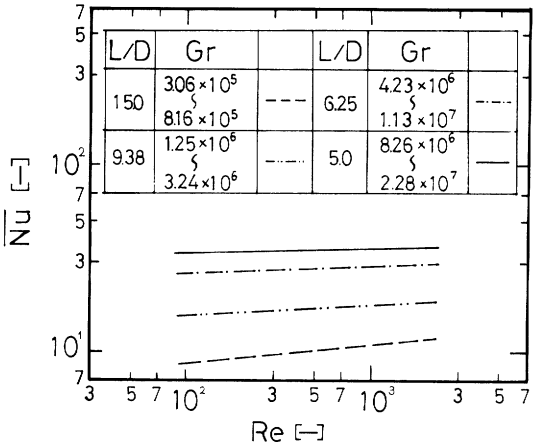

Fig. 9 Relation between calculated $\overline{Nu}$ and *Re*

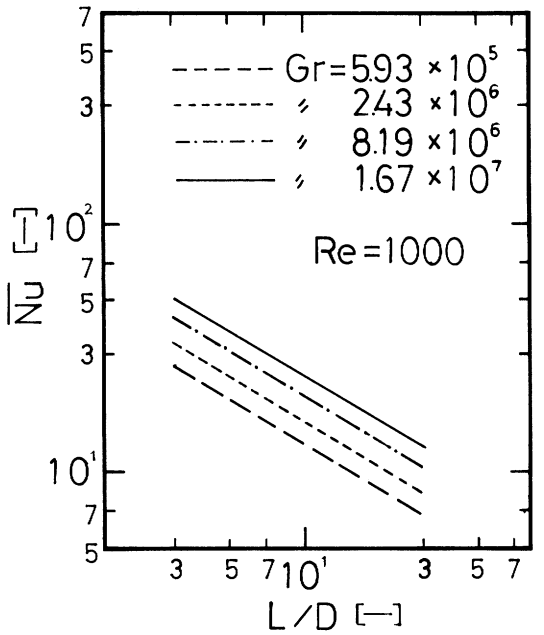

Fig. 10 Relation between calculated $\overline{Nu}$ and *L/D*

4. Effect of Operating Conditions on Heat Transfer Coefficient

The relations between average Nusselt number from the heated surface in the duct and *Re*, *Gr* and *L/D* were investigated by numerical calculations.

Figure 9 shows the relation between *Re* and calculated $\overline{Nu}$ with *Gr* as a parameter. From Fig. 9, as *Re* is increased, $\overline{Nu}$ slightly increases. This means that the effect of forced convection on $\overline{Nu}$ is very weak. From these calculated results, $\overline{Nu}$ was proportional to about $Re^{0.055}$.

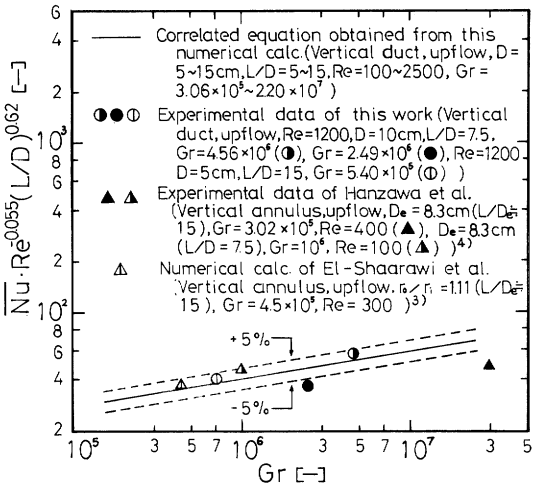

Fig. 11 Relation between $NuRe^{-0.055}(L/D)^{0.62}$ and Gr

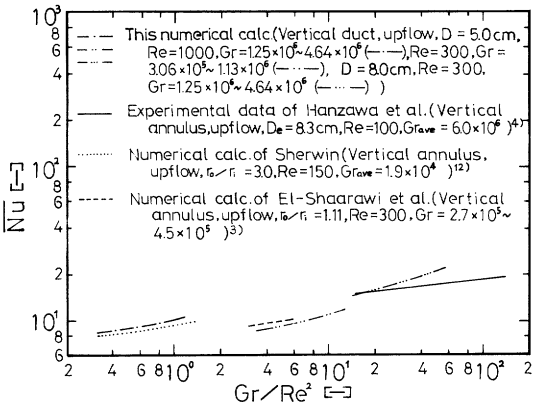

Fig. 12 Average Nu compared with some previous results

Figure 10 shows the relation between L/D and $\overline{Nu}$ with Gr as a parameter. From Fig. 10, when L/D is increased, $\overline{Nu}$ decreases. This means that $\overline{Nu}$ is affected sensitively by L/D and also decreases with decreasing D. This tendency was also obtained in other cases. From these calculated results, $\overline{Nu}$ was proportional to $(L/D)^{-0.62}$. Furthermore, $\overline{Nu}$ was also affected by Gr and was proportional to $Gr^{0.18}$.

Figure 11 shows the relationship between Gr and $\overline{Nu}\,(Re)^{-0.055}\,(L/D)^{0.62}$. From Fig. 11, the following correlated equation was obtained within a difference of ±5 % at the most for the heat transfer coefficient in a vertical duct with an isothermal heating section and upward forced-convective flow.

$$\overline{Nu} = 4.3(Re)^{0.055} Gr^{0.18} (L/D)^{-0.62} \tag{8}$$

In Fig. 11, the plotted points show experimental values from the present study and some previous results[3, 4] for $\overline{Nu}$ for a vertical heated surface in a flow system similar to that used by the authors.

From Fig. 11, it seems that the experimental values can be explained well by this correlated equation, and that Eq. (8) is a fairly good approximation.

The applicable ranges of Eq. (8) are from 100 to 2500 for Re, 3.09×10^5 to 2.2×10^7 for Gr and 5.0 to 15.0 for L/D.

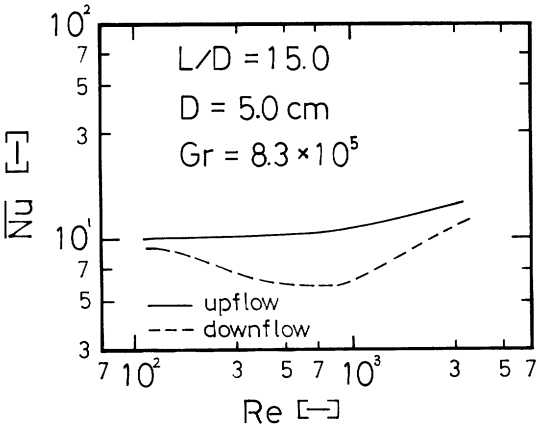

Fig. 13 Comparison of $\overline{Nu}$ with upflow system and downflow systemstem

5. Discussion

Figure 12 shows some typical relationships between $\overline{Nu}$ and the free-forced convective flow rate. The abscissa of the figure represents Gr/Re^2 and the ordinate represents $\overline{Nu}$.

From Fig. 12, $\overline{Nu}$ increases slowly with increasing Gr/Re^2 in the whole range. Figure 12 also shows some previous results for $\overline{Nu}$ for a vertical heated surface in a flow system similar to that used by the authors. From this figure, there is a reasonable correlation of values of $\overline{Nu}$ between the upflow systems of Sewin[12], El—Shaarawi *et al.*[3] and Hanzawa *et al.*[4] and the present one.

In this system, the free convective flow generated near a heated wall is upward and is reinforced by forced convective flow in the same direction in the laminar flow range. Therefore, it is assumed that the heat transfer rates increase by reinforcing flow which is combined with these two flows in the case of upflow.

Figure 13 shows typical comparisons of $\overline{Nu}$ in the upflow system and the downflow system in the previous study[5, 6] for L/D = 15.0 and $Gr = 8.3 \times 10^5$. From Fig. 13, it appears that $\overline{Nu}$ in the downflow system is considerably smaller than that in the present upflow system, and there is a reduction by half in the value of $\overline{Nu}$ between the downflow system and the present one in the range of about Re = 300 – 1500.

Conclusions

As basic research on the effect of the direction of cold fluid flow on the cooling of the package, velocity and temperature distributions were investigated for the case where one wall of the vertical duct was isothermally heated and gas flowed upward through the duct in the laminar flow range as a model of the package wall in

a refrigerating room. The fundamental equations were solved numerically to analyze the heat transfer in the duct. To check these calculated results, the temperature distributions were measured experimentally under the same operating conditions as those of the theoretical analysis. The following results were obtained.

(1) Free convective flow generated near the heated wall is reinforced by the upward forced convective flow.

(2) Calculated streamlines and temperature distributions agreed closely with visualized streamlines and measured temperature distributions.

(3) The local Nusselt number near the heated wall increased rapidly near the bottom of the heated wall and decreased gradually with increasing axial distance.

(4) A correlated equation for the heat transfer coefficient in a vertical duct (with an isothermal heating section and upflow) was obtained within the limits of this investigation.

Nomenclature

C_p	=	heat capacity at constant pressure	[J/g·K]
D	=	plate spacing	[cm]
Gr	=	Grashof number (= $g\beta D^3 (t_H - t_0)/\nu^2$)	[-]
g	=	gravitational acceleration	[cm/s^2]
H	=	height of duct	[cm]
h	=	local heat transfer coefficient	[W/cm^2·K]
L	=	height of heated wall	[cm]
Nu	=	Nusselt number (= $h \cdot D/\lambda$)	[-]
P	=	pressure	[Pa]
Pr	=	Prandtl number (= $C_p \cdot \mu/\lambda$)	[-]
Re	=	Reynolds number (= $D \cdot \bar{v}/\nu$)	[-]
T	=	dimensionless temperature (= $(t - t_0)/(t_H - t_0)$)	[-]
t	=	temperature	[K]
U	=	dimensionless velocity in X-direction (= $u \cdot D/\nu$)	[-]
u	=	velocity in x-direction	[cm/s]
V	=	dimensionless velocity in Y-direction (= $v \cdot D/\nu$)	[-]
v	=	velocity in y-direction	[cm/s]
X	=	dimensionless horizontal distance (= x/D)	[-]
x	=	horizontal coordinate	[cm]
Y	=	dimensionless horizontal distance (= y/D)	[-]
Y_H	=	dimensionless height of duct (= H/D)	[-]
y	=	axial coordinate	[cm]
β	=	volumetric coefficient of expansion of fluid	[K^{-1}]
ξ	=	dimensionless vorticity	[-]
ΔX	=	dimensionless grid size in x-direction	[-]
ΔY	=	dimensionless grid size in y-direction	[-]
λ	=	thermal conductivity of fluid	[W/cm·K]
μ	=	viscosity of fluid	[Pa·s]
ν	=	kinematic viscosity of fluid	[cm^2/s]
ρ	=	density of fluid	[g/cm^3]
ψ	=	dimensionless stream function	[-]

<Subscripts>

A	=	lower end of heated wall
B	=	upper end of heated wall
H	=	heating zone
M	=	middle point of heating zone
W	=	wall
0	=	inlet zone

<Superscripts>

—	=	average

Literature Cited

1) Chow, L. C., S.R. Husain and A. Campo: *J. Heat Transfer*, **106**, 297-303 (1984)
2) Colwell, R. G. and J.R. Welty: *J. Heat Transfer*, **96**, 448-454 (1974)
3) El-Shaarawi, M. A. I. and A. Sarhan: *J. Heat Transfer*, **102**, 617-622 (1980)
4) Hanzawa, T., A. Sako and K. Kato: *J. Chem. Eng. Japan*, **19**, 96-103 (1986)
5) Hanzawa, T., H.T. Yu, Y.T. Hsiao and N. Sakai: *J. Chem. Eng. Japan*, **24**, 726-730 (1991)
6) Hanzawa, T., Y.T. Hsiao, H.T. Yu and N. Sakai: J. Chem. *Eng. Japan*, **25**, 307-314 (1992)
7) Kemeny, G. A. and E.V. Somers: *J. Heat Transfer*, **84**, 339-346 (1962)
8) Kitamura, K. and T. Inagaki: *Int. J. Heat Mass Transfer*, **30**, 23-41 (1987)
9) Mabuchi, I.: *Nihon Kikai Gakkai Ronbunshu*, **26**, 720-725 (1960)
10) Miyatake, O. and T. Fujii: *Kagaku Kogaku*, **36**, 405-412 (1972)
11) Miyatake, O. and T. Fujii: *Kagaku Kogaku*, **37**, 491-496 (1973)
12) Oosthuizen, P.H. and R. Hart: *J. Heat Transfer*, **95**, 60-63 (1973)
13) Serwin, K.: *British Chem. Eng.*, **13**, 569-574 (1968)
14) Szewczyk, A.A.: *J. Heat Transfer*, **86**, 501-507 (1964)
15) Tanaka, H., S. Maruyama and S. Hatano: *Int. J. Heat Mass Trasnfer*, **30**, 165-173 (1987)
16) Tao, L.N.: *J. Heat Transfer*, **82**, 233-238 (1960)
17) Umino, K., Y. Nagasawa, H. Hanzawa, N. Takahashi and H. Tajima: *J. Takenaka Tech. Report*, **31**, 27-36 (1984)
18) Yamaguchi, K., Y. Inoue, K. Yoneyama and A. Yoshikawa: *Kukichowa Eisei Kogaku Ronbunshu*, **52**, 85-95 (1978)
19) Zeldin, B. and F. W. Schmidt: *J. Heat Transfer*, **94**, 211-223 (1972)